

Human-AI Collaborative Multi-modal Multi-rater Learning for Endometriosis Diagnosis

Hu Wang, David Butler, Yuan Zhang, Jodie Avery, Steven Knox, Congbo Ma, Louise Hull, Gustavo Carneiro

The University of Adelaide, Adelaide, Australia
Benson Radiology, Adelaide, Australia
Macquarie University, Sydney, Australia
University of Surrey, Guildford, United Kingdom

Abstract. Endometriosis, affecting about 10% of individuals assigned female at birth, is challenging to diagnose and manage. Diagnosis typically involves the identification of various signs of the disease using either laparoscopic surgery or the analysis of T1/T2 MRI images, with the latter being quicker and cheaper but less accurate. A key diagnostic sign of endometriosis is the obliteration of the Pouch of Douglas (POD). However, even experienced clinicians struggle with accurately classifying POD obliteration from MRI images, which complicates the training of reliable AI models. In this paper, we introduce the Human-AI Collaborative Multi-modal Multi-rater Learning (HAICOMM) methodology to address the challenge above. HAICOMM is the first method that explores three important aspects of this problem: 1) multi-rater learning to extract a cleaner label from the multiple “noisy” labels available per training sample; 2) multi-modal learning to leverage the presence of T1/T2 MRI images for training and testing; and 3) human-AI collaboration to build a system that leverages the predictions from clinicians and the AI model to provide more accurate classification than standalone clinicians and AI models. Presenting results on the multi-rater T1/T2 MRI endometriosis dataset that we collected to validate our methodology, the proposed HAICOMM model outperforms an ensemble of clinicians, noisy-label learning models, and multi-rater learning methods.

1. Introduction

Endometriosis is characterized by the abnormal growth of endometrial-like tissue outside the uterus, often leading to distressing symptoms such as chronic pain, prolonged menstrual bleeding, and infertility [1, 2]. Despite its prevalence in around 10% of individuals assigned female at birth [3], diagnosing endometriosis has been a hard condition to diagnose. Conventional diagnostic methods primarily rely on invasive laparoscopy, a surgical procedure that involves the insertion of a slender camera through a small incision in the abdomen to visually inspect the pelvic region [4]. This diagnostic method, while effective, presents substantial drawbacks. Chief among them is the significant delay (averaging 6.4 years [3]) that patients endure before receiving a formal

diagnosis. This long waiting period lowers the quality of life for those afflicted by the condition [5]. Furthermore, the extensive reliance on laparoscopy escalates healthcare costs, imposing a considerable burden on both healthcare systems and patients [6]. These challenges underscore the pressing need for innovative imaging-based diagnostic solutions that can mitigate these issues while enhancing patient care.

The T1 and T2 modalities of Magnetic Resonance Imaging (MRI) are among the most recommended medical imaging methods for diagnosing endometriosis given their effectiveness to visualize many signs of the condition. One of the most important signs associated with the condition is the Pouch of Douglas (POD) Obliteration [7, 8]. Developing an AI model capable of classifying POD obliteration has the potential to facilitate the widespread adoption of imaging-based diagnosis and enhance diagnosis accuracy and consistency. However, training such a model relies on acquiring precise POD Obliteration annotations from T1/T2 MRIs, which is a challenging task because even experienced clinicians may lack certainty regarding the presence of the sign. In fact, the uncertainty in the manual POD obliteration classification from T1/T2 MRI is remarkably low, with only 61.4% to 71.9% accuracy [9, 10]. Nevertheless, there have been some attempts at training such multi-modal MRI AI models for classifying POD obliteration, such as Zhang et al.’s [11] method to distill the POD obliteration classification knowledge from ultrasound to MRI, or Butler et al. [8]’s self-supervised pre-training for multi-modal POD obliteration classification. However, none of these methods have been tested against ground truth labels obtained from surgery reports, so it is hard to assess if their published accuracy results are competitive with purely manual classifications. Therefore, a major research question in this problem is if it is possible to design innovative training and testing methodologies that can lead to highly accurate POD obliteration classification results.

There are many important aspects of this problem that can be leveraged in order to formulate an innovative solution to produce an accurate POD obliteration classifier. First, the uncertain manual classification by clinicians can lead to training sets that contain multiple “noisy” labels per training sample (with each label being produced by a different clinician), which can be explored by multi-rater learning mechanisms [12]. Second, given that clinicians and AI models may not be highly accurate, the combination of their predictions may lead to more accurate predictions – such idea is studied by human-AI collaborative classification [13]. Third, similarly to previous approaches [11, 8], it is important to explore the complementarity of the multiple MRI modalities.

In this paper, we explore the three points listed above to propose the innovative Human-AI Collaborative Multi-modal Multi-rater Learning (HAICOMM) methodology. HAICOMM is the first method in the field that simultaneously explores multi-rater learning to provide a clean training label from the multiple “noisy” labels produced by clinicians, multi-modal learning to leverage the presence of T1/T2 MRI images, and human-AI collaboration to build a system that synergises predictions from both clinicians and the AI model. The contributions of this paper are:

- The first human-AI collaborative multi-modal multi-rater learning methodology that produces a highly accurate POD obliteration classifier from T1/T2 MRIs;
- The first multi-modal multi-rater dataset annotated with imaging and surgery-based POD obliteration labels for the diagnosis of endometriosis.

Experiments on our proposed endometriosis dataset shows that our HAICOMM model presents more accurate POD classification than predictions produced by an ensemble of clinicians, by noisy-label learning methods, and by multi-rater learning methods.

2. Literature Review

2.1. Human-AI Collaboration

Human-AI Collaboration (HAIC) integrates the unique strengths of human experts and AI systems, resulting in improved model capabilities and performance when compared to standalone AI systems [14, 15]. The motivation behind HAIC arises from research [16, 17, 18] that highlights the limitations of traditional isolated AI methods, overlooking the potential of human-AI collaboration. To overcome these limitations, researchers have proposed various strategies to enhance human-AI collaboration [19, 20, 21, 22]. Two key strategies within HAIC have emerged: learning to defer and learning to complement. Learning to defer (L2D), which evolved from the concept of learning to reject [23, 24], focuses on optimizing the decision of whether to defer prediction to either the expert or the AI system. Researchers have investigated several L2D approaches [25, 26, 27], initially in single-expert scenarios but later extending to multi-user collaborations [28, 29, 30]. On the other hand, learning to complement [13] focuses on maximizing the expected utility of combined human-AI decisions, and various frameworks have been proposed to model human-AI complementarity [31, 32, 33, 19, 34].

2.2. Multi-modal Learning

Multi-modal learning has become increasingly crucial in various fields, including medical image analysis and computer vision. It combines data from different sources to provide a more comprehensive understanding of tasks. In medical image analysis, several innovative methods have been developed. These include a chilopod-shaped architecture using modality-dependent feature normalization and knowledge distillation [35], a pixel-wise coherence approach modeling aleatoric uncertainty [36], a trusted multi-view classifier using the Dirichlet distribution [37], and an uncertainty-aware model based on cross-modal random network prediction [38]. Computer vision has seen advancements in multi-modal learning as well. Researchers have combined channel exchanging with multi-modal learning [39], applied self-supervised learning to improve performance [40, 41], enhanced video-and-sound source localization [42], introduced a model for multi-view learning [43], and explored feature disentanglement methods [44, 45].

2.3. Multi-rater Learning

Multi-rater learning is a technique designed to train a classifier using noisy labels gathered from multiple annotators. The challenge lies in how to derive a “clean” label from these imperfect labels. Traditional approaches often rely on majority voting [46] and the expectation-maximization (EM) algorithm [47, 48]. Rodrigues et al. [49] introduce an end-to-end deep neural network (DNN) that incorporates a crowd layer to model the annotator-specific transition matrix, enabling the direct training of a DNN with crowdsourced labels. Alternatively, Chen et al. [50] suggest a probabilistic model that learns an interpretable transition matrix unique to each annotator. Meanwhile, Guan et al. [51] employ multiple output layers in the classifier and learn combination weights to aggregate the results. More recently, CROWDLAB [52] has set the state of the art in multi-rater learning by using multiple noisy-label samples and predictions with a model trained via label noise learning. Despite the promise of multi-rater learning in leveraging multiple noisy labels per training sample, it falls short by overlooking the concept of human-AI collaboration and multi-modal learning.

2.4. Imaging-based Endometriosis Detection

One crucial indicator to detect endometriosis is the obliteration of the Pouch of Douglas (POD) [7, 8]. However, the development of an AI model that can classify such indicator hinges on the availability of precise POD obliteration annotations from T1/T2 MRIs, a task that is challenging because even experienced clinicians often face uncertainty in identifying this sign. Despite these challenges, there have been some efforts to train multi-modal MRI AI models for POD obliteration classification. For example, Zhang et al. [11] proposed a method to transfer knowledge from ultrasound to MRI for classifying POD obliteration, and Butler et al. [8] explored self-supervised pre-training for multi-modal POD obliteration classification. However, these methods have not been validated against ground-truth labels obtained from surgical reports, making it difficult to determine if their reported accuracy is truly competitive with manual classification.

Nevertheless, for all of the aforementioned related work, none of the methods deal with human-AI collaboration, multi-modal classification, and multi-rater learning simultaneously, particularly for classifying endometriosis. In this paper, we propose the HAICOMM model to address this research gap.

3. Methodology

The training of our HAICOMM methodology is depicted in Fig. 1. The first stage consists of pre-training a multi-modal encoder using a large unlabelled T1/T2 MRI dataset, with a self-supervised learning mechanism [53] (see frame (a) in Fig. 1). Subsequently, for training the proposed human-AI classifier HAICOMM, we first need to estimate the pseudo ground truth label from the the multiple “noisy” labels available for each pair of T1/T2 MRI training images. We rely on CrowdLab [12] to produce such

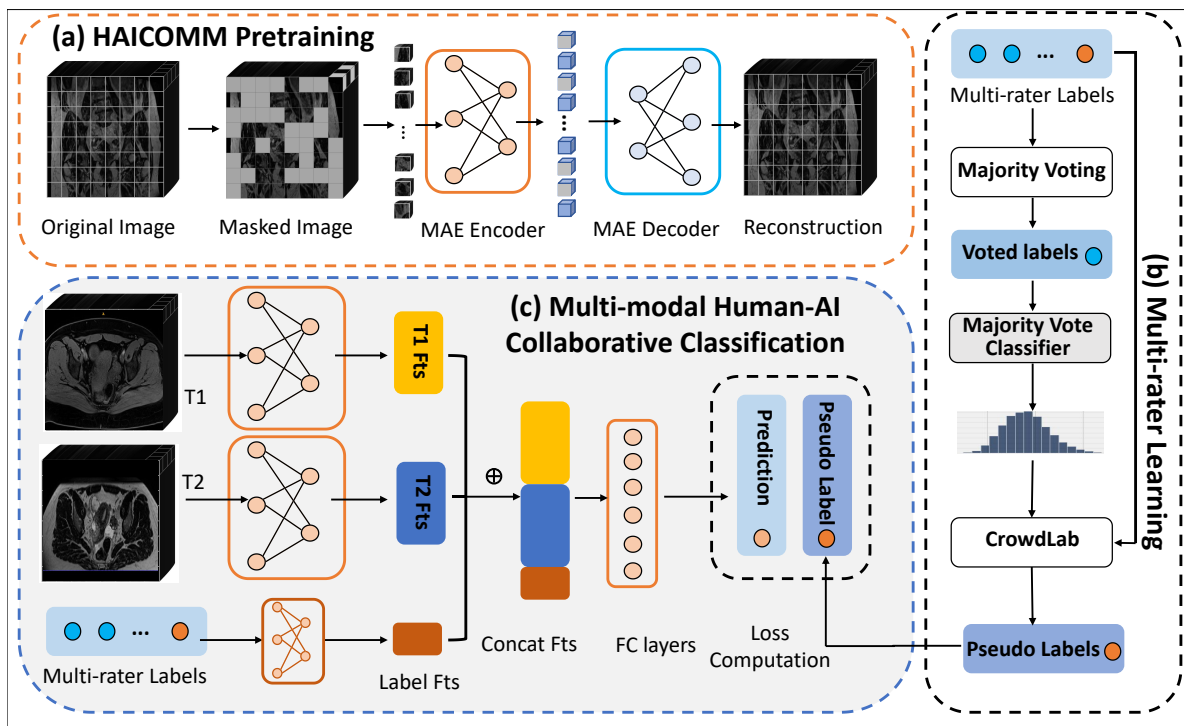


Figure 1. The framework of HAICOMM. The MRI encoders of HAICOMM are: (a) firstly pre-trained with a Masked Autoencoder (MAE) model; then (b) the pseudo clean labels are estimated from the multi-rater learning process; next, (c) the T1 and T2 data, along with the human-produced multi-rater labels are entered into respective feature extraction encoders – the features from three sources are fused for the final prediction. In the figure, “FC” means fully-connected. “Fts” represents features. “Concat” presents concatenation and “ \oplus ” denotes the concatenation operation.

pseudo ground truth labels (see frame (b) in Fig. 1). Next, the T1/T2 MRI images with multi-rater (manual) labels are fed into their multi-modal encoders. The embeddings from the multi-modal and label encoders are combined to produce the final prediction that is trained to match the pseudo ground truth label (see frame (c) in Fig. 1). We provide details about each of these training stages below.

3.1. Multi-modal Encoder Pre-training

The MRI encoder of the HAICOMM model is pre-trained with the Masked Autoencoder (MAE) self-supervised learning method [53]. For this pre-training, we use a dataset denoted as $\mathcal{D}_P = \{\mathbf{x}_{t1}^{(i)}\}_{i=1}^{M_{t1}} \cup \{\mathbf{x}_{t2}^{(i)}\}_{i=1}^{M_{t2}}$, with $\mathbf{x}_{t1}^{(i)}, \mathbf{x}_{t2}^{(i)} \in \mathcal{X} \subset \mathbb{R}^{H \times W \times D}$ denoting the T1 and T2 MRI volumes of size $H \times W \times D$. It is worth noting that the number of unlabeled images, $M = M_{t1} + M_{t2}$, far exceeds the number of labeled images, denoted as N (i.e., $M \gg N$), of the datasets that will be defined in Sections 3.2 and 3.3.

Following the 3D Vision Transformer [54], the architecture of 3D-MAE follows an asymmetric encoder-decoder setup. The encoder, parameterized by ϕ , is represented by $g_\phi : \mathcal{X} \rightarrow \mathcal{F}$, which receives visible patches along with positional embeddings that

are processed through a 3D Vision Transformer to produce features in the space \mathcal{F} . The resulting features are subsequently directed to the decoder, parameterized by ψ and denoted by $f_\psi : \mathcal{F} \rightarrow \mathcal{X}$, which reconstructs the original volume with the masked volume tokens. In the MRI pre-training, our objective is to minimize the mean squared error (MSE) of the reconstruction of the original masked patches. Formally, we have:

$$\phi^*, \psi^* = \arg \min_{\phi, \psi} \frac{1}{M} \left(\sum_{i=1}^{M_{t1}} \|f_\psi(g_\phi(\mathbf{x}'_{t1})) - \mathbf{x}'_{t1}\|_2^2 + \sum_{i=1}^{M_{t2}} \|f_\psi(g_\phi(\mathbf{x}'_{t2})) - \mathbf{x}'_{t2}\|_2^2 \right), \quad (1)$$

where $\|\cdot\|_2$ denotes the L2-norm. For the training and evaluation of the human-AI collaborative classifier, we use the feature extractor $g_{\phi^*}(\cdot)$, as explained below in Sec. 3.3.

3.2. Multi-rater Learning

The training of our human-AI collaborative classifier requires each pair of T1/T2 MRI training images to have a single pseudo clean label estimated from the multiple “noisy” training labels. The multi-modal multi-rater dataset is denoted by $\mathcal{D}_T = \{(\mathbf{x}_{t1}^{(i)}, \mathbf{x}_{t2}^{(i)}, \mathbf{y}^{(i)})\}_{i=1}^N$ with N samples, where the multi-rater label has K binary annotations denoted as $\mathbf{y}^{(i)} \in \mathcal{Y} \subset \{0, 1\}^K$, provided by the K clinicians who annotated the training images in \mathcal{D}_T .

With the multi-rater labels, we first perform majority vote to fetch the most frequently appearing labels per training sample. Let us present the majority vote operation as $h : \mathcal{Y} \rightarrow \{0, 1\}$. Then, we have the mapping from multi-rater labels to the majority label for each multi-modal sample. As a result, we can form a new dataset with

$$\mathcal{D}_{MV} = \{(\mathbf{x}_{t1}^{(i)}, \mathbf{x}_{t2}^{(i)}, \hat{y}^{(i)})\}_{i=1}^N, \text{ where } \hat{y}^{(i)} = h(\mathbf{y}^{(i)}), \quad (2)$$

where $\hat{y}^{(i)} \in \{0, 1\}$. With such generated consensus labels from majority vote, we train a classifier $f_\theta : \mathcal{X} \times \mathcal{X} \rightarrow [0, 1]$ that takes the T1 and T2 MRI volumes to optimize a standard binary cross-entropy objective. This classifier, together with \mathcal{D}_T will then be used to train the multi-rater learning method CrowdLab [12], denoted by $z : [0, 1] \times \mathcal{Y} \rightarrow \{0, 1\}$, which generates a pseudo clean label for each sample. Formally, this pseudo labeling process can be defined by:

$$y^{(i)} = z(f_\theta(\mathbf{x}_{t1}^{(i)}, \mathbf{x}_{t2}^{(i)}), \mathbf{y}^{(i)}), \quad (3)$$

where $y^{(i)} \in \{0, 1\}$ denotes CrowdLab’s estimate for the “clean” label of the i -th sample, which is referred to as the pseudo ground-truth label.

3.3. Multi-modal Human-AI Collaborative Classification

Given the pseudo clean labels $y^{(i)}$ from (3), the dataset for model training is defined as:

$$\mathcal{D}'_T = \{(\mathbf{x}_{t1}^{(i)}, \mathbf{x}_{t2}^{(i)}, \mathbf{y}^{(i)}, y^{(i)})\}_{i=1}^N. \quad (4)$$

The pre-trained encoder from (1), parameterized by ϕ^* , is utilized to initialize the T1 and T2 MRI feature extractors, respectively defined by $g_{\hat{\phi}} : \mathcal{X} \rightarrow \mathcal{F}$ and $g_{\phi'} : \mathcal{X} \rightarrow \mathcal{F}$,

for the classification task. We also need to define a new feature extractor for processing the manual labels with a learnable module defined as $g_\gamma : \mathcal{Y} \rightarrow \mathcal{F}$. Such manual labels are used in the human-AI collaborative module.

Hence, these feature extractors produce:

$$\mathbf{F}_{t1}^{(i)} = g_{\hat{\phi}}(\mathbf{x}_{t1}^{(i)}), \mathbf{F}_{t2}^{(i)} = g_{\phi'}(\mathbf{x}_{t2}^{(i)}), \mathbf{F}_r^{(i)} = g_\gamma(\mathbf{y}^{(i)}). \quad (5)$$

These three feature maps are then concatenated and fed into a learnable linear projection $\pi_\eta : \mathcal{F} \times \mathcal{F} \times \mathcal{F} \rightarrow \mathcal{F}$, parameterized by η to predict:

$$\mathbf{p}^{(i)} = \sigma \left(\pi_\eta(\mathbf{F}_{t1}^{(i)} \oplus \mathbf{F}_{t2}^{(i)} \oplus \mathbf{F}_r^{(i)}) \right), \quad (6)$$

where $\mathbf{p}^{(i)} \in [0, 1]^2$ denotes the probabilistic prediction, \oplus represents the concatenation operator, and σ is the softmax function. Finally, the training of the whole model is performed by minimizing the binary cross-entropy loss, as follows:

$$\hat{\phi}^*, \phi'^*, \gamma^*, \eta^* = \arg \min_{\hat{\phi}, \phi', \gamma, \eta} -\frac{1}{N} \left(\sum_{i=1}^N y^{(i)} \log(p^{(i)}) + (1 - y^{(i)}) \log(1 - p^{(i)}) \right), \quad (7)$$

where the $p^{(i)}$ is the predicted probability of the positive class of i -th sample (i.e., the 2nd dimension $\mathbf{p}^{(i)}$ in (6)), and $y^{(i)}$ is the pseudo clean label in \mathcal{D}'_T .

The testing process consists of taking the input T1/T2 MRI images and labels \mathbf{y} from clinicians to output \mathbf{p} from (6).

4. Experiments

4.1. Endometriosis Dataset

We first introduce our multi-modal multi-rater dataset annotated with imaging and surgery-based POD obliteration labels for the diagnosis of endometriosis. For the pre-training stage, we collected 5,867 unlabeled T1 MRI volumes and 8,984 unlabeled T2 MRI volumes from patients aged between 18 and 45 years old, where the volumes show female pelvis scans obtained from various MRI machines with varying resolutions. To standardize the data, the volumes were resampled to $1\text{mm} \times 1\text{mm} \times 3\text{mm}$ voxels. Also, we apply 3D contrast-limited adaptive histogram equalization (CLAHE) to enhance image local contrast and refine edge definitions.

For the training of the human-AI collaborative POD obliteration classifier, we collected 82 pairs of T1/T2 MRI volumes with patients aged 18 to 45 years old. These scans were obtained across multiple clinical sites, with each case annotated by three experienced clinicians who work in clinics specialized in the imaging-based diagnosis of endometriosis. The scans show a specific region surrounding the uterus, which is the area where the signs of POD obliteration are more visible. We further collect 30 cases that contain ground truth annotation of POD obliteration from surgical reports. These cases serve as gold standards for testing. We also use CLAHE pre-processing in this dataset.

4.2. Implementation Details

For model pre-training, the input volumes are either cropped or zero-padded to achieve dimensions of $64 \times 128 \times 128$ voxels. To maintain consistency with the pre-training dataset, the endometriosis training samples are cropped in the uterine region at the same dimensions as pre-training data, i.e. $64 \times 128 \times 128$ voxels. In both pre-training and the training of the human-AI collaborative POD obliteration classifier, the multi-modal encoder for each modality is a transformer with 12 blocks. The majority vote classifier has a 3D-ResNet50 as its backbone network [55]. For the human-AI collaborative POD obliteration classifier training, we use 5 epochs for model optimization warming up. AdamW optimizer and base learning rate of 1e-3 with cosine annealing [56] learning rate tuning strategy are adopted. Three multi-rater labels from three different annotators are incorporated into the training process. In the testing phase, the scans are also cropped in the uterine regions and the clinical surgical results serve as the ground truth for accurate evaluation. All of our models are trained for 60 epochs without model selection. Note that the majority voting is only produced for the consensus pseudo label required for the training of the model $f_{\theta}(\cdot)$ to be used by CrowdLab, as explained in Eq. 3. Once the pseudo clean labels are generated by CrowdLab, the majority voting will no longer be needed.

4.3. Quantitative Evaluation Settings

We compare the performance of our proposed HAICOMM with respect to the following models: 1) purely manual annotation from the three expert clinicians via majority voting; 2) models trained with noisy-label learning techniques (SSR [57] and ProMix [58]) using the noisy labels from one of the annotators (GT1, GT2, GT3); 3) models trained from labels produced by the multi-rater learning CrowdLab [12] (in the table denoted as models w/ CL); and 4) human-AI classifiers using the three annotators (models w/ HAIC). In terms of evaluation metrics, we adopt Accuracy and Area Under the ROC Curve (AUROC).

4.4. Overall Performance

The performance results in Table 1 show that the proposed HAICOMM outperforms other competing models by a large margin across the accuracy and AUC measures. Relative improvements vary from 9.10% to 54.83% on accuracy and 19.37% and 64.75% on AUROC. The standard deviation is calculated by inference time bootstrapping.

There are interesting points to observe in the results from Table 1. First, the multi-rater learning tends to be more accurate than noisy label learning. The manual annotation without any assistance from the model $f_{\theta}(\cdot)$ in Eq. 3, shows a relatively low accuracy of 0.7, motivating the importance of the proposed human-AI collaboration. Also, when noisy-label learning models are designed to collaborate with humans, we can see large performance improvements, such as shown by “SSR w/ HAIC” and “ProMix

Table 1. The performance comparison of HAICOMM and other models in terms of test accuracy and AUROC (and respective improvements of HAICOMM) with the testing ground-truth labels from surgical reports. “Majority Vote” denotes a purely manual classification using the majority vote of the three annotators. SSR and ProMix w/ “GT1”, “GT2” and “GT3” mean noisy-label learning models trained with labels from annotators #1, #2 and #3, respectively. “CL” denotes noisy-label learning models trained with labels $y^{(i)}$ from Eq. (3) produced by the multi-rater learning method CrowdLab. “HAIC” represents a model that collaborates with the annotators and that is trained with labels from CrowdLab. The best results for each column are in bold.

Methods	Models	Accuracy	Improvement	AUROC	Improvement
Human	Majority Vote	0.7000±0.0000	14.29%	-	-
Noisy Label Learning	SSR w/ GT1	0.5833±0.0236	37.93%	0.5763±0.0121	53.83%
	SSR w/ GT2	0.6000±0.0408	33.33%	0.5845±0.0112	51.67%
	SSR w/ GT3	0.5667±0.0157	41.17%	0.5644±0.0572	57.07%
	ProMix w/ GT1	0.5333±0.0236	50.01%	0.5381±0.0412	64.75%
	ProMix w/ GT2	0.6167±0.0314	29.72%	0.5808±0.0151	52.63%
	ProMix w/ GT3	0.5167±0.0471	54.83%	0.5663±0.0245	56.54%
Multi- rater	SSR w/ CL	0.6167±0.0236	29.72%	0.5878±0.0078	50.82%
	ProMix w/ CL	0.6500±0.0408	23.08%	0.5428±0.0328	63.32%
HAIC	SSR w/ HAIC	0.6833±0.0849	17.08%	0.7424±0.0047	19.37%
	ProMix w/ HAIC	0.6667±0.0624	20.00%	0.7389±0.0367	19.98%
Ours	HAICOMM	0.8000±0.0408	-	0.8865±0.0551	-

w/ HAIC”. However, the proposed HAICOMM still obtains much higher accuracy and AUROC. Additionally, the proposed HAICOMM shows a much simpler training algorithm than “SSR w/ HAIC” and “ProMix w/ HAIC”. To summarize, the proposed model outperforms not only the ensemble of experts (Majority Vote), but also the top-performing multi-rater learning model (SSR w/CL and ProMix w/ CL), as well as the best noisy-label learning methods (SSR and ProMix), even after adding human AI collaboration (SSR w/ HAIC and ProMix w/ HAIC) by a large margin.

4.5. Human-AI Collaborative Multi-modal Multi-rater Ablation Study

In this subsection, we show an ablation study of different combinations of annotators to be used in the human-AI collaboration and model training. We also analyze the use of multi-modal data in the results.

The first three rows of Table 2 present the accuracy of each of the three annotators. The next rows show HAICOMM without relying on any human collaboration (w/o HAIC), then the next 6 rows show different combinations of annotators for the human-AI collaboration process. This is followed by two rows showing HAICOMM with single modality data (either T1 or T2) in the input. Last row shows the HAICOMM results. Note that the collaboration with annotators almost always improve over the result of HAICOMM w/o HAIC, and it also improves the accuracy for most of the annotators

Table 2. Accuracy and AUROC performance analyses of HAICOMM and its variants. “R1”, “R2” and “R3” denote models trained with input annotations from annotators #1, #2 and #3, respectively. “HAIC” represents model trained with multi-rater labels inputs for human-AI collaborations. T1 and T2 Only w/ HAIC represent single-modality HAICOMM approaches. The best results for each column are in bold.

Models	Accuracy	AUROC
Labels from Rater #1 (R1)	0.6667	-
Labels from Rater #2 (R2)	0.7333	-
Labels from Rater #3 (R3)	0.7000	-
HAICOMM w/o HAIC	0.6333	0.5933
HAICOMM w/ R1	0.7667	0.7044
HAICOMM w/ R2	0.8000	0.8444
HAICOMM w/ R3	0.5667	0.5956
HAICOMM w/ R1,2	0.7667	0.8667
HAICOMM w/ R2,3	0.7333	0.8711
HAICOMM w/ R1,3	0.6333	0.6689
T1 Only w/ HAIC	0.6667	0.8067
T2 Only w/ HAIC	0.7667	0.8844
HAICOMM	0.8000	0.8865

(particularly R1 and R2). Interestingly, we found that the model with R2 inputs performs the best among with single rater labels. The model with combination inputs of R1 and R3 performs the worst. This may suggest that R2 provides relatively more accurate labels compared to R1 and R3. This phenomenon resonates with the fact that R2 provides the most accurate labels among three raters (as shown in the first three rows). This table also shows that both single modality results with HAIC (with T2 being much better than T1) have worse results than the multi-modal HAICOMM, which provides evidence of the need for multi-modal analysis in the classification of POD obliteration.

5. Qualitative Analyses

We also conduct qualitative analyses about HAICOMM. In Figure 2, (a) and (b) are the input T1 and T2 MRIs, respectively. The table below shows the predictions by the three raters (Rater #1,#2,#3), then the predictions by SSR and ProMix trained with Rater #1’s labels and CROWDLAB’s labels (SSR w GT1, ProMix w GT1, SSR w CL GT, ProMix w CL GT). Next, we show SSR and ProMix trained with CROWDLAB’s labels and relying on human-AI collaborative classification (SSR w HAIC, ProMix w HAIC), followed by the result from our HAICOMM, and the ground truth label from surgical data. The case shows the proposed HAICOMM model can generate correct labels while

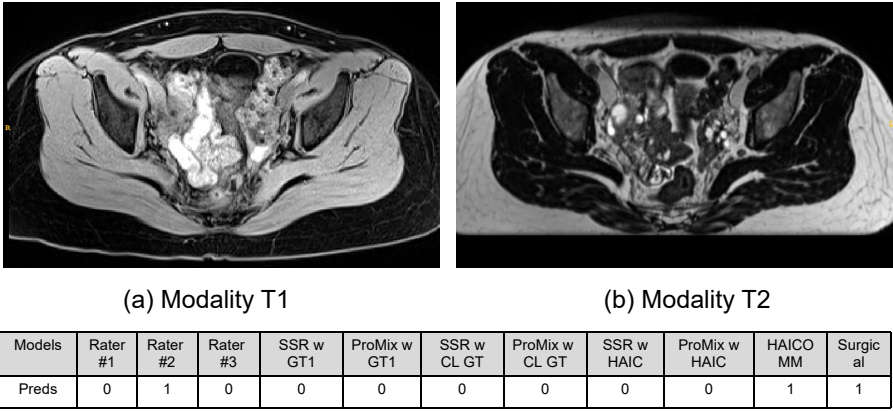


Figure 2. Qualitative results of HAICOMM.

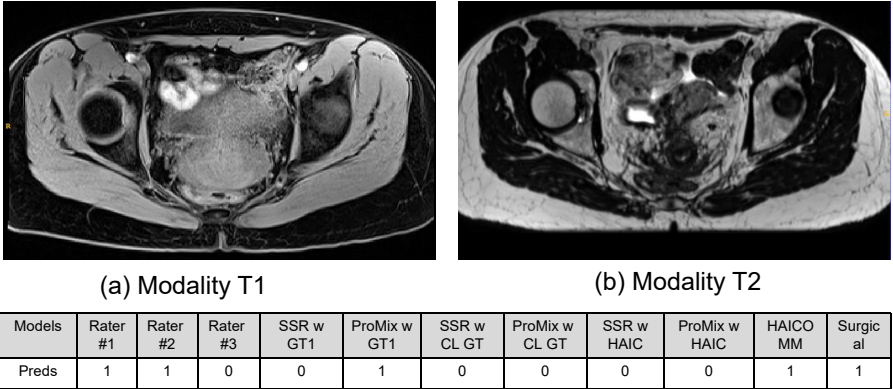


Figure 3. Another qualitative result of HAICOMM.

other models cannot. For 3, the case also shows that the proposed HAICOMM model can generate a correct label while most other methods cannot (only ProMix w GT1 and HAICOMM predict the surgical ground truth label correctly).

6. Conclusion and Future Work

In this paper, we proposed the Human-AI Collaborative Multi-modal Multi-rater Learning (HAICOMM) methodology for an imaging-based endometriosis classification. It integrates the capabilities of machine learning models and multiple human labels to enhance the classification accuracy of POD obliteration from T1/T2 MRIs. Evaluation on our endometriosis dataset demonstrates the efficacy of the HAICOMM model, surpassing ensemble clinician predictions, noisy-label learning approaches, and a multi-rater learning method. This underscores the potential of collaborative efforts between AI and human clinicians in diagnosing and managing endometriosis and other complex medical conditions. To the best of knowledge, we are the first to propose the multi-modal multi-rater classification task. Furthermore, our endometriosis dataset is the first

in the field to enable the development of multi-modal multi-rater classifiers.

One potential limitation of our method is the dataset size. Currently, we are dedicated to collect more data from different clinical sources to expand the dataset. The use of such multiple clinical sources will require the exploration of domain adaptation techniques to enable a better flexibility of the method to work in multiple domains. Beyond this issue, the need for specific labellers for training and testing is another potential limitation. We plan to address this issue with the development of techniques that work with a variable set of labellers during training and testing. Another interesting direction is the collection of new datasets for other multi-modal multi-rater clinical problems to enable the evaluation of our HAICOMM in a different task.

References

- [1] A. S. Lagana, F. M. Salmeri, H. Ban Frangež, F. Ghezzi, E. Vrtačnik-Bokal, R. Granese, Evaluation of m1 and m2 macrophages in ovarian endometriomas from women affected by endometriosis at different stages of the disease, *Gynecological Endocrinology* 36 (5) (2020) 441–444.
- [2] K. Moss, J. Doust, H. Homer, I. Rowlands, R. Hockey, G. Mishra, Delayed diagnosis of endometriosis disadvantages women in art: a retrospective population linked data study, *Human Reproduction* 36 (12) (2021) 3074–3082.
- [3] A. I. of Health, Welfare, Endometriosis in Australia: Prevalence and Hospitalisations: In Focus, Australian Institute of Health and Welfare, 2019.
- [4] C. M. Becker, et al., Eshre guideline: endometriosis, *Human reproduction open* 2022 (2) (2022) hoac009.
- [5] A. W. Horne, S. A. Missmer, Pathophysiology, diagnosis, and management of endometriosis, *bmj* 379 (2022).
- [6] A. M. Soliman, H. Yang, E. X. Du, C. Kelley, C. Winkel, The direct and indirect costs associated with endometriosis: a systematic literature review, *Human reproduction* 31 (4) (2016) 712–722.
- [7] K. Kinkel, K. A. Frei, C. Balleyguier, C. Chapron, Diagnosis of endometriosis with imaging: a review, *European radiology* 16 (2006) 285–298.
- [8] D. Butler, H. Wang, Y. Zhang, M.-S. To, G. Condous, M. Leonardi, S. Knox, J. Avery, L. Hull, G. Carneiro, The effectiveness of self-supervised pre-training for multi-modal endometriosis classification*†, 2023 45th Annual International Conference of the IEEE Engineering in Medicine & Biology Society (EMBC) (2023) 1–5.
URL <https://api.semanticscholar.org/CorpusID:266196804>
- [9] M. L. Kataoka, et al., Posterior cul-de-sac obliteration associated with endometriosis: Mr imaging evaluation, *Radiology* 234 (3) (2005) 815–823.
- [10] T. Indrielle-Kelly, et al., Diagnostic accuracy of ultrasound and mri in the mapping of deep pelvic endometriosis using the international deep endometriosis analysis (idea) consensus, *BioMed research international* 2020 (2020).
- [11] Y. Zhang, H. Wang, D. Butler, M.-S. To, J. Avery, M. L. Hull, G. Carneiro, Distilling missing modality knowledge from ultrasound for endometriosis diagnosis with magnetic resonance images, in: 2023 IEEE 20th International Symposium on Biomedical Imaging (ISBI), IEEE, 2023. doi:10.1109/isbi53787.2023.10230667.
URL <http://dx.doi.org/10.1109/ISBI53787.2023.10230667>
- [12] H. W. Goh, U. Tkachenko, J. Mueller, C. C. Cleanlab, Crowdlab: Supervised learning to infer consensus labels and quality scores for data with multiple annotators, *arXiv preprint arXiv:2210.06812* (2022).
- [13] B. Wilder, E. Horvitz, E. Kamar, Learning to complement humans, in: Proceedings of the Twenty-Ninth International Joint Conference on Artificial Intelligence, IJCAI’20, 2021.

- [14] Z. Lu, M. Yin, Human reliance on machine learning models when performance feedback is limited: Heuristics and risks, in: Proceedings of the 2021 CHI Conference on Human Factors in Computing Systems, 2021, pp. 1–16.
- [15] K. Weitz, D. Schiller, R. Schlagowski, T. Huber, E. André, ” do you trust me?” increasing user-trust by integrating virtual agents in explainable ai interaction design, in: Proceedings of the 19th ACM International Conference on Intelligent Virtual Agents, 2019, pp. 7–9.
- [16] A. Rosenfeld, M. D. Solbach, J. K. Tsotsos, Totally looks like-how humans compare, compared to machines, 2018, pp. 1961–1964.
- [17] T. Serre, Deep learning: the good, the bad, and the ugly, Annual review of vision science 5 (2019) 399–426.
- [18] E. Kamar, S. Hacker, E. Horvitz, Combining human and machine intelligence in large-scale crowdsourcing., in: AAMAS, Vol. 12, 2012, pp. 467–474.
- [19] G. Bansal, B. Nushi, E. Kamar, E. Horvitz, D. S. Weld, Is the most accurate ai the best teammate? optimizing ai for teamwork, in: AAAI, Vol. 35, 2021, pp. 11405–11414.
- [20] K. Vodrahalli, R. Daneshjou, T. Gerstenberg, J. Zou, Do humans trust advice more if it comes from ai? an analysis of human-ai interactions, in: Proceedings of the 2022 AAAI/ACM Conference on AI, Ethics, and Society, 2022, pp. 763–777.
- [21] X. Wu, L. Xiao, Y. Sun, J. Zhang, T. Ma, L. He, A survey of human-in-the-loop for machine learning, Future Gener. Comput. Syst. 135 (C) (2022) 364–381. doi:10.1016/j.future.2022.05.014.
URL <https://doi.org/10.1016/j.future.2022.05.014>
- [22] M. F. Pradier, J. Zazo, S. Parbhoo, R. H. Perlis, M. Zazzi, F. Doshi-Velez, Preferential mixture-of-experts: Interpretable models that rely on human expertise as much as possible, AMIA Summits on Translational Science Proceedings 2021 (2021) 525.
- [23] C. Cortes, G. DeSalvo, M. Mohri, Learning with rejection, in: Algorithmic Learning Theory: 27th International Conference, ALT 2016, Bari, Italy, October 19–21, 2016, Proceedings 27, Springer, 2016, pp. 67–82.
- [24] D. Madras, T. Pitassi, R. Zemel, Predict responsibly: improving fairness and accuracy by learning to defer, NeurIPS 31 (2018).
- [25] H. Narasimhan, W. Jitkrittum, A. K. Menon, A. Rawat, S. Kumar, Post-hoc estimators for learning to defer to an expert, NeurIPS 35 (2022) 29292–29304.
- [26] M. Raghu, K. Blumer, G. Corrado, J. Kleinberg, Z. Obermeyer, S. Mullainathan, The algorithmic automation problem: Prediction, triage, and human effort, arXiv preprint arXiv:1903.12220 (2019).
- [27] N. Okati, A. De, M. Rodriguez, Differentiable learning under triage, NeurIPS 34 (2021) 9140–9151.
- [28] R. Verma, D. Barrejón, E. Nalisnick, On the calibration of learning to defer to multiple experts, in: Workshop on Human-Machine Collaboration and Teaming in International Conference of Machine Learning, 2022.
- [29] A. Mao, C. Mohri, M. Mohri, Y. Zhong, Two-stage learning to defer with multiple experts, in: NeurIPS, 2023.
- [30] P. Hemmer, S. Schellhammer, M. Vössing, J. Jakubik, G. Satzger, Forming effective human-ai teams: Building machine learning models that complement the capabilities of multiple experts, International Joint Conferences on Artificial Intelligence Organization, 2022, pp. 2478–2484, main Track. doi:10.24963/ijcai.2022/344.
URL <https://doi.org/10.24963/ijcai.2022/344>
- [31] M. Steyvers, H. Tejada, G. Kerrigan, P. Smyth, Bayesian modeling of human-ai complementarity, Proceedings of the National Academy of Sciences 119 (11) (2022) e2111547119.
- [32] G. Kerrigan, P. Smyth, M. Steyvers, Combining human predictions with model probabilities via confusion matrices and calibration, NeurIPS 34 (2021) 4421–4434.
- [33] Z. Zhang, K. Wells, G. Carneiro, Learning to complement with multiple humans (lecomh): Integrating multi-rater and noisy-label learning into human-ai collaboration, arXiv preprint

- arXiv:2311.13172 (2023).
- [34] M. Liu, J. Wei, Y. Liu, J. Davis, Do humans and machines have the same eyes? human-machine perceptual differences on image classification, arXiv preprint arXiv:2304.08733 (2023).
 - [35] Q. Dou, Q. Liu, P. A. Heng, B. Glocker, Unpaired multi-modal segmentation via knowledge distillation, in: *IEEE Transactions on Medical Imaging*, 2020.
 - [36] M. Monteiro, L. Le Folgoc, D. Coelho de Castro, N. Pawlowski, B. Marques, K. Kamnitsas, M. van der Wilk, B. Glocker, Stochastic segmentation networks: Modelling spatially correlated aleatoric uncertainty, *Advances in Neural Information Processing Systems* 33 (2020) 12756–12767.
 - [37] Z. Han, C. Zhang, H. Fu, J. T. Zhou, Trusted multi-view classification, arXiv preprint arXiv:2102.02051 (2021).
 - [38] H. Wang, J. Zhang, Y. Chen, C. Ma, J. Avery, L. Hull, G. Carneiro, Uncertainty-aware multi-modal learning via cross-modal random network prediction, in: *European Conference on Computer Vision*, Springer, 2022, pp. 200–217.
 - [39] Y. Wang, W. Huang, F. Sun, T. Xu, Y. Rong, J. Huang, Deep multimodal fusion by channel exchanging, *Advances in Neural Information Processing Systems* 33 (2020) 4835–4845.
 - [40] M. Patrick, Y. M. Asano, P. Kuznetsova, R. Fong, J. F. Henriques, G. Zweig, A. Vedaldi, Multi-modal self-supervision from generalized data transformations, arXiv preprint arXiv:2003.04298 (2020).
 - [41] M. Patrick, P.-Y. Huang, I. Misra, F. Metze, A. Vedaldi, Y. M. Asano, J. F. Henriques, Space-time crop & attend: Improving cross-modal video representation learning, in: *Proceedings of the IEEE/CVF International Conference on Computer Vision*, 2021, pp. 10560–10572.
 - [42] H. Chen, W. Xie, T. Afouras, A. Nagrani, A. Vedaldi, A. Zisserman, Localizing visual sounds the hard way, in: *Proceedings of the IEEE/CVF Conference on Computer Vision and Pattern Recognition*, 2021, pp. 16867–16876.
 - [43] X. Jia, X.-Y. Jing, X. Zhu, S. Chen, B. Du, Z. Cai, Z. He, D. Yue, Semi-supervised multi-view deep discriminant representation learning, *IEEE transactions on pattern analysis and machine intelligence* 43 (7) (2020) 2496–2509.
 - [44] H.-Y. Lee, H.-Y. Tseng, J.-B. Huang, M. Singh, M.-H. Yang, Diverse image-to-image translation via disentangled representations, in: *Proceedings of the European conference on computer vision (ECCV)*, 2018, pp. 35–51.
 - [45] X. Liu, P. Sanchez, S. Thermos, A. Q. O’Neil, S. A. Tsiftaris, Learning disentangled representations in the imaging domain, *Medical Image Analysis* (2022) 102516.
 - [46] Z.-H. Zhou, *Ensemble methods: foundations and algorithms*, CRC press, 2012.
 - [47] F. Rodrigues, F. Pereira, B. Ribeiro, Gaussian process classification and active learning with multiple annotators, in: *ICML*, PMLR, 2014, pp. 433–441.
 - [48] V. C. Raykar, S. Yu, L. H. Zhao, G. H. Valadez, C. Florin, L. Bogoni, L. Moy, Learning from crowds., *Journal of machine learning research* 11 (4) (2010).
 - [49] F. Rodrigues, F. Pereira, *Deep learning from crowds*, Vol. 32, 2018.
 - [50] Z. Chen, H. Wang, H. Sun, P. Chen, T. Han, X. Liu, J. Yang, Structured probabilistic end-to-end learning from crowds, 2021, pp. 1512–1518.
 - [51] M. Guan, V. Gulshan, A. Dai, G. Hinton, Who said what: Modeling individual labelers improves classification, in: *AAAI*, Vol. 32, 2018.
 - [52] H. W. Goh, U. Tkachenko, J. Mueller, Crowdlab: Supervised learning to infer consensus labels and quality scores for data with multiple annotators (2023). arXiv:2210.06812.
 - [53] K. He, X. Chen, S. Xie, Y. Li, P. Dollár, R. Girshick, Masked autoencoders are scalable vision learners, in: *Proceedings of the IEEE/CVF conference on computer vision and pattern recognition*, 2022, pp. 16000–16009.
 - [54] A. Dosovitskiy, et al., An image is worth 16x16 words: Transformers for image recognition at scale, arXiv preprint arXiv:2010.11929 (2020).
 - [55] K. Hara, H. Kataoka, Y. Satoh, Learning spatio-temporal features with 3d residual networks for

- action recognition, in: Proceedings of the IEEE international conference on computer vision workshops, 2017, pp. 3154–3160.
- [56] I. Loshchilov, F. Hutter, Sgdr: Stochastic gradient descent with warm restarts, arXiv preprint arXiv:1608.03983 (2016).
- [57] C. Feng, G. Tzimiropoulos, I. Patras, SSR: an efficient and robust framework for learning with unknown label noise, in: 33rd British Machine Vision Conference 2022, BMVC 2022, London, UK, November 21-24, 2022, BMVA Press, 2022, p. 372.
URL <https://bmvc2022.mpi-inf.mpg.de/372/>
- [58] R. Xiao, Y. Dong, H. Wang, L. Feng, R. Wu, G. Chen, J. Zhao, Promix: combating label noise via maximizing clean sample utility, in: Proceedings of the Thirty-Second International Joint Conference on Artificial Intelligence, IJCAI-23, E. Elkind, Ed. International Joint Conferences on Artificial Intelligence Organization, Vol. 8, 2023, pp. 4442–4450.